

Investigation of two- and three-nucleon transfer reactions in $^{12}\text{C} + ^{56}\text{Fe}$

HARI S PATEL, B SRINIVASAN, B J ROY and M G BETIGERI
Nuclear Physics Division, Bhabha Atomic Research Centre, Mumbai 400 085, India
Email: mgb@magnum.barc.ernet.in

MS received 15 June 1998

Abstract. Multi-nucleon transfer reactions $^{56}\text{Fe}(^{12}\text{C}, \text{X})$ have been studied at an incident ^{12}C energy of 60 MeV. Angular distributions of ^{10}Be and ^9Be corresponding to $2p$ and $2p1n$ transfer reactions in transition to low-lying states in the residual nuclei have been measured. The angular distribution data for $2p$ transfer have been analysed in terms of finite range DWBA calculations assuming a one-step transfer of two protons. The spectroscopic factors for three low-lying transitions observed in $^{56}\text{Fe}(^{12}\text{C}, ^{10}\text{Be})^{58}\text{Ni}$ have been extracted. Transfer probabilities for the ground state transition in two- and three-nucleon stripping channels have been obtained and compared with the corresponding sequential transfer probabilities in order to emphasise the role of direct transfer of nucleons vis-a-vis sequential transfer.

Keywords. Nuclear reactions $^{56}\text{Fe}(^{12}\text{C}, ^{12}\text{C})$, $(^{12}\text{C}, ^{10}\text{Be})$, $(^{12}\text{C}, ^9\text{Be})$; $E = 60$ MeV; measured angular distributions; deduced S; transfer probabilities; reaction mechanisms.

PACS No. 25.70

1. Introduction

The dissipation of energy and angular momentum in a heavy ion induced reaction is generally understood to proceed by emission of a number of nucleons. Depending on the reaction mechanism, the origin of multi-nucleon transfer could be due to direct transfer of nucleons involving their single particle nature and/or other effects due to pairing, clustering etc. [1]. On the other hand, a fused system could form and, depending on the mass asymmetry, a number of nucleons would evaporate sequentially following statistical decay of such a fused system [2]. The multi-nucleon transfer between two complex nuclei often occurs with a probability comparable to that of one nucleon transfer and accounts for a large fraction of the total reaction cross-section. In spite of considerable progress, the mechanism involved in multi-nucleon transfer is not very well understood. The presence of multi-step transfer involving sequential transfer, inelastic excitations prior or after the transfer etc., in addition to the usually dominant direct cluster transfer complicates the reaction mechanism. The motivation behind some of our recent experiments [3, 4, 5] on $^{12}\text{C} + ^{115}\text{In}$ and $^{12}\text{C} + ^{88}\text{Sr}$ has been to understand the reaction mechanism involved in single- and multi-nucleon transfer to discrete low lying states [3, 4] and also to the continuum [5].

In order to further investigate these aspects, the nucleus ^{56}Fe close to the doubly closed shell ($Z = 28, N = 28$) has been chosen as a target for the present investigation. Earlier studies on two proton stripping reaction leading to the proton shell closed ($Z = 28$) nucleus ^{58}Ni have been reported using light ions mainly [6, 7]. The reaction mechanism in $^{56}\text{Fe}(^{12}\text{C}, ^{10}\text{Be})^{58}\text{Ni}$ leading to discrete low-lying states in the residual nucleus ^{58}Ni has not been studied.

The reaction ($^{12}\text{C}, ^9\text{Be}$) provides a simple channel for studying three nucleon correlations in nuclei. Alpha clustering in nuclei has been well studied through transfer reactions involving light as well as heavy ions. However, the mechanism involved in three nucleon transfer reactions in the collision between two heavy ions has not been well studied and no data are available for the reaction $^{56}\text{Fe}(^{12}\text{C}, ^9\text{Be})^{59}\text{Ni}$.

The present work reports on the study of two- and three-nucleon transfer reactions on $^{12}\text{C} + ^{56}\text{Fe}$ at $E(^{12}\text{C}) = 60$ MeV. The details of the results are discussed.

2. Experimental details

The experiment was carried out with a ^{12}C beam obtained from the 14UD Pelletron accelerator at Mumbai, India. The target was a self supporting natural iron (abundance of ^{56}Fe in $^{\text{nat}}\text{Fe}$ is 91.72%) foil of thickness $\approx 275 \mu\text{m}/\text{cm}^2$. Reaction products were detected and identified by three counter telescopes, each consisting of a $30 \mu\text{m}$ thick silicon surface-barrier ΔE detector placed in front of an E -detector ($\approx 300 \mu\text{m}$). A fast-slow coincidence set-up with a time resolution of ≈ 8 ns helped to reduce chance coincidence rates and to achieve a clean charge and mass separation of the light reaction products (figure 1). The standard particle identification algorithm was used to identify the reaction products.

3. Results and analysis

An excitation function study ^{10}Be and ^9Be outgoing channels corresponding to two- and three-nucleon transfer reactions was carried out at incident ^{12}C energies ranging from 60 to 77 MeV. The study shows (figure 2) that although cross-section for the data integrated over the entire excitation energy range for the two- and three-nucleon transfer channels increases with increase in the projectile energy, the $^9\text{Be}(^{10}\text{Be})$ production cross-section, integrated up to 5 MeV, falls by a factor of 20(3), when the bombarding energy is increased from 60 to 77 MeV. This fall can be understood as due to the effect of shifting of the optimum Q -value from a value close to the ground state Q -value at $E(^{12}\text{C}) = 60$ MeV to a high negative value $= -18$ MeV at $E(^{12}\text{C}) = 77$ MeV. Since the interest in the present work was to study the low lying discrete transitions in the two- and three-nucleon transfer reactions, the measurements were carried out at $E(^{12}\text{C}) = 60$ MeV.

The energy spectrum of ^{10}Be and ^9Be measured at $\theta_{\text{lab}} = 19^\circ$ is shown in figure 3. Several discrete transitions have been observed in the two proton transfer channel of which the first three peaks at $E_x = 0.0, 1.45$ and 2.45 MeV have been identified as the $0^+, 2^+$ and 4^+ states, respectively, in ^{58}Ni [8]. It was not possible to identify the

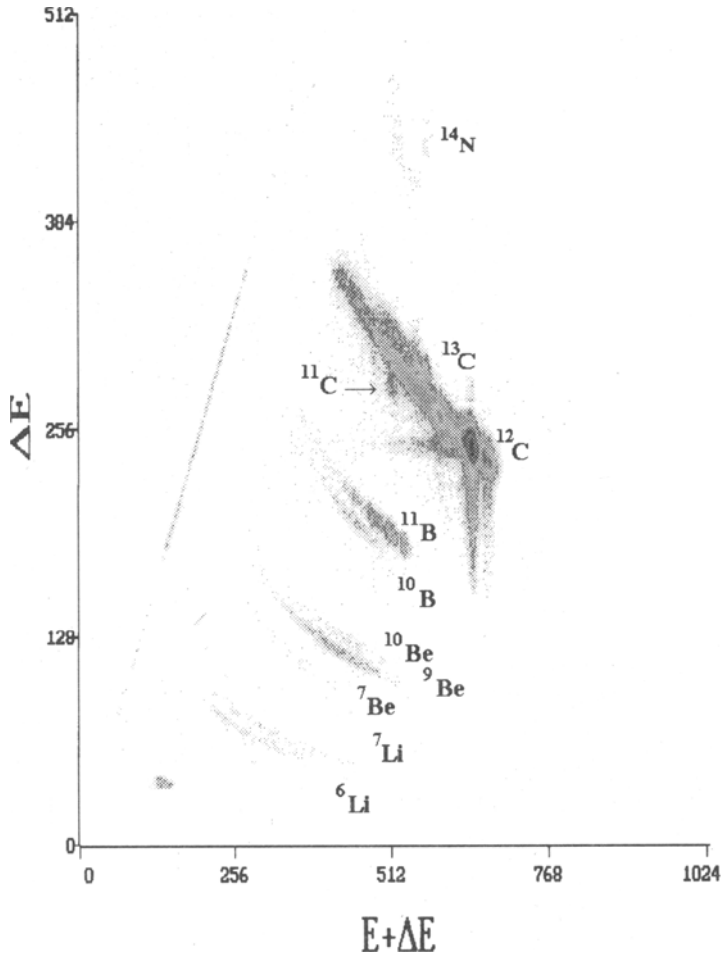


Figure 1. Mass spectrum (ΔE versus $E + \Delta E$) in $^{56}\text{Fe}(^{12}\text{C}, X)$ at $E_{\text{inc}} = 60$ MeV and $\theta_{\text{lab}} = 19^\circ$.

other peaks seen at higher excitation energy as a number of states exist in ^{58}Ni in this excitation range and the energy resolution (≈ 500 keV) achieved in the present experiment was not sufficient to resolve the individual transitions. The angular distributions for the lowest three transitions have been studied from $\theta_{\text{lab}} = 11^\circ$ to 32.5° .

In the three particle transfer reaction $^{56}\text{Fe}(^{12}\text{C}, ^9\text{Be})^{59}\text{Ni}$, a clear peak at $E_x = 0$ MeV has been observed (figure 3). Three low-lying close levels within 500 keV excitation exist in ^{59}Ni [9] which within the resolution achieved in the present experiment cannot be separated. The peak seen at $E_x = 0$ MeV is thus due to the addition of the contributions from the $\frac{3}{2}^-$ (g.s.), $\frac{5}{2}^-$ (343 keV) and $\frac{1}{2}^-$ (468 keV) states. No effort has been made to analyse the groups seen at higher excitation energy as it was not possible to associate them with individual transitions. Angular distribution for the above group at $E_x = 0$ MeV has been measured in the range of $\theta_{\text{lab}} = 11^\circ$ to 32.5° .

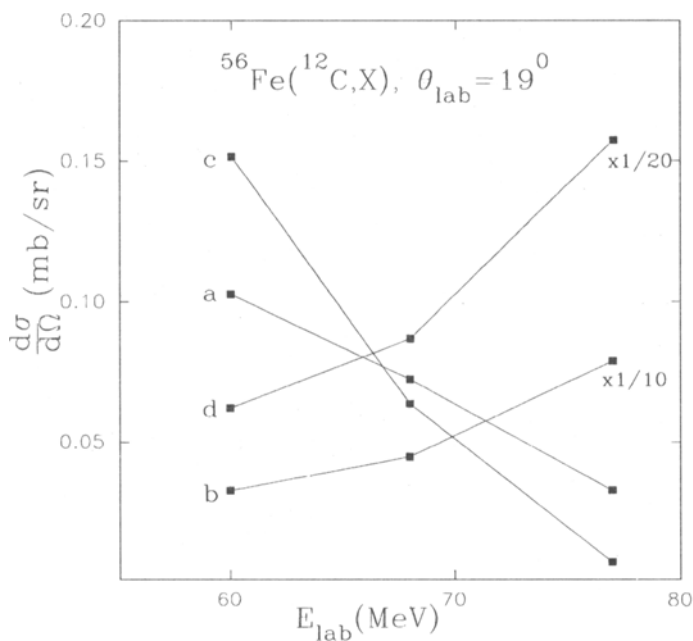


Figure 2. Differential cross-section for $^{56}\text{Fe}(^{12}\text{C},^{10}\text{Be})$ integrated up to 5 MeV excitation (a) and integrated over the entire excitation (b) in ^{58}Ni plotted as a function of the projectile energy. Similarly the excitation function for $^{56}\text{Fe}(^{12}\text{C},^9\text{Be})$ integrated up to 5 MeV excitation (c) and integrated over the entire excitation (d) in ^{59}Ni are also shown. Solid lines are drawn through the data points to guide the eye.

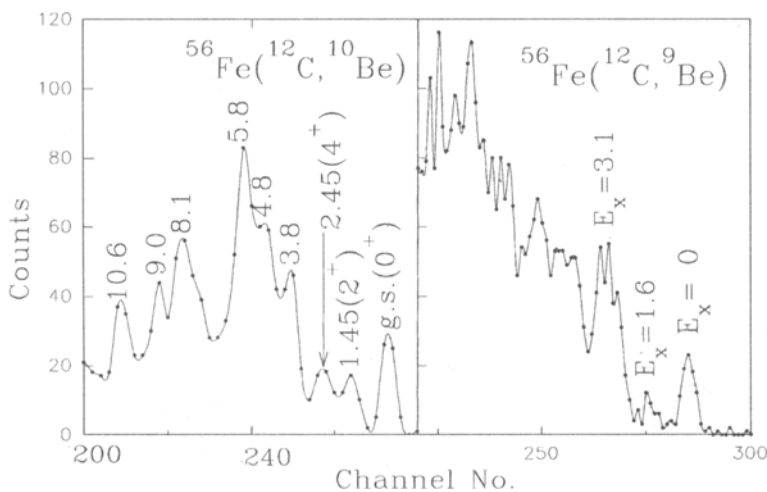


Figure 3. Energy spectra of ^{10}Be and ^9Be in $^{56}\text{Fe}(^{12}\text{C}, X)$ reaction at $E(^{12}\text{C}) = 60$ MeV and $\theta_{\text{lab}} = 19^\circ$. Excitation energies indicated in the figure are in MeV.

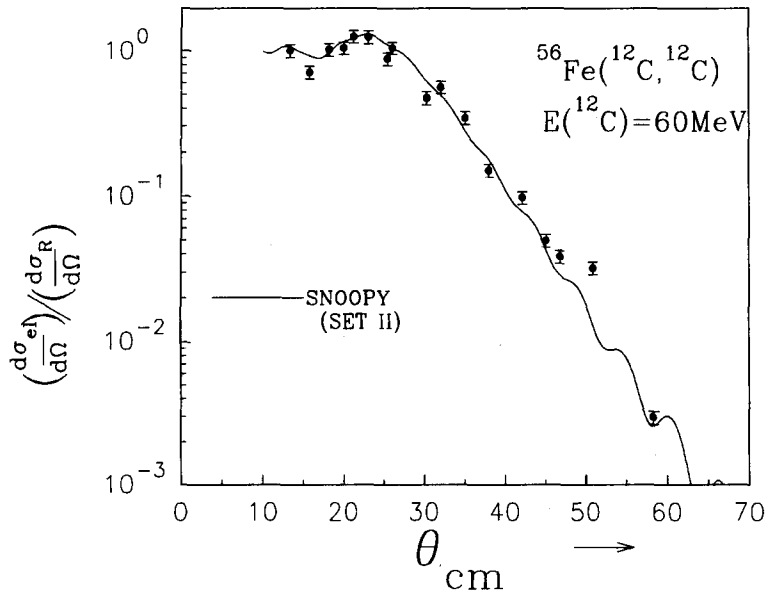


Figure 4. The ratio of elastic scattering to the Rutherford cross-section for $^{12}\text{C} + ^{56}\text{Fe}$ at 60 MeV. Fit shown is the optical model calculation using SNOOPY.

3.1 DWBA analysis

The measured angular distributions for the $0^+ \rightarrow 0^+$, $0^+ \rightarrow 2^+$ and $0^+ \rightarrow 4^+$ transitions observed in ($^{12}\text{C}, ^{10}\text{Be}$) reactions have been analysed using the finite range DWBA code LOLA assuming a one-step direct transfer of two protons. The two protons were assumed to be in a relative $S = 0$ and $T = 1$ state while being transferred. The two proton cluster wave function was calculated in a Woods-Saxon well with $r_0 = 1.25$ fm, $a_0 = 0.65$ fm and the depth was adjusted to reproduce the experimental two-proton separation energies. The transferred di-proton was assumed to go into the $f_{7/2}$ orbit [7].

In order to calculate distorted waves needed in the DWBA calculations, the elastic scattering angular distribution for the system $^{12}\text{C} + ^{56}\text{Fe}$ at $E(^{12}\text{C}) = 60$ MeV has been measured and the optical model potential has been derived by fitting the measured data with an optical model search code SNOOPY [10]. The measured elastic scattering angular distribution is shown in figure 4. The shape of the angular distribution is typical of Fresnel scattering with an almost exponential fall beyond $\theta > \theta_{\text{grazing}} = 33^\circ$. The starting proximity potential (set I of table 1) leads to a final set of parameters (set II of table 1) for which a best fit to the data (figure 4) was obtained.

The optical model potential (set II of table 1) has been used in the DWBA calculations to calculate the distorted waves for the incoming channel. However, for the outgoing channel i.e., for $^{10}\text{Be} + ^{58}\text{Ni}$, the potential parameters were varied to obtain a fit to the transfer data. The resulting set of parameters is also listed in table 1. The LOLA results normalised to the experimental data at forward angles are shown in figure 5 along with the measured angular distributions. The calculated angular distributions provide satisfactory fit to the data over the limited angular range of measurements. The pronounced

Table 1. Optical model potential parameters.

SET	V	r_0	a_0	W	r_i	a_i	Comments
I	49.0	1.2	0.62	15.0	1.2	0.62	
II	48.0	1.191	0.643	12.0	1.191	0.634	$^{12}\text{C} + ^{56}\text{Fe}$
III	50.0	1.3	0.70	12.0	1.191	0.643	$^{10}\text{Be} + ^{58}\text{Ni}$

oscillations seen for the ground state transition is typical of $L = 0$ transfer. Oscillations are damped for the 2^+ and 4^+ angular distributions and can be understood as due to the effect of contributions from several magnetic substates for a non-zero angular momentum transfer.

Assuming a value of $C^2S_a = 1.98$ for the overlap $|\langle ^{12}\text{C} | ^{10}\text{Be} + 2p \rangle|^2$ [11], spectroscopic factors for the levels in ^{58}Ni relative to the g.s. (0^+) have been derived by comparison between the experimental cross-sections and DWBA predictions and are presented in table 2. When the values are normalised to the only reported [7] spectroscopic factor for the $^{56}\text{Fe}(^3\text{He},n)^{58}\text{Ni}(0^+)$, a value of $S = 0.47$ for the 2^+ and $S = 0.62$ for the 4^+ state is obtained.

3.2 Analysis in terms of transfer probability

In heavy ion induced multi-nucleon transfer reactions, a number of mechanisms of different complexity, viz., cluster transfer, sequential transfer etc., can contribute to a

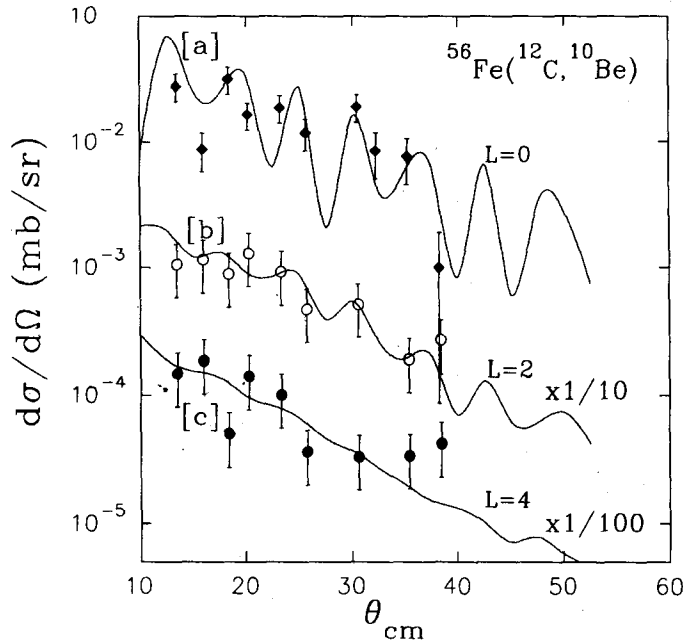


Figure 5. Angular distribution of $^{56}\text{Fe}(^{12}\text{C}, ^{10}\text{Be})$ for transition to (a) 0^+ (g.s.), (b) 2^+ (1.45 MeV), and (c) 4^+ (2.4 MeV) states in ^{58}Ni . The solid lines are the finite range DWBA calculations using LOLA.

Table 2. The two-proton spectroscopic factors in ^{58}Ni deduced from the present measurement.

Ex(MeV)	J^π	Relative $S^{\text{a)}}$	Absolute $S^{\text{b)}}$
0.0	0^+	1.0	0.94
1.45	2^+	0.50	0.47
2.45	4^+	0.66	0.62

^{a)} Relative to the ground state is the present measurement.

^{b)} On normalising to the spectroscopic factor for the ground state given in ref. [7].

given transition. The multi-step sequential transfer, in some cases, can compete with the one-step cluster transfer and may become a dominant mechanism. While the measured angular distributions indicate qualitatively the nature of the reaction mechanism involved, any quantitative evaluation is non-trivial. In order to emphasise the role of simultaneous transfer of correlated nucleons vis-a-vis multi-step sequential transfer in the present two- and three-nucleon transfer reactions, an approach based on the transfer probability considerations followed in the literature [4, 12, 13] has been used in the present work. The transfer probability, P_{tr} , is defined as the ratio of transfer cross-section to elastic scattering cross-section measured simultaneously. The experimentally measured transfer probabilities for multi-nucleon transfer when compared with the corresponding probabilities for multi-step sequential transfer, also measured experimentally, may indicate the importance of direct cluster transfer of nucleons. P_{tr} for two/three-nucleon transfer have been derived from the present measurement and have been compared with the corresponding sequential probabilities as detailed below.

The mechanism for two proton transfer may involve (a) simultaneous transfer of a proton pair and (b) sequential transfer of two protons which is a two-step process. As is mentioned in ref. [13] P_{tr} must be calculated for a well defined state, the P_{2p} in the present study was computed from the experimental data for the $0^+ \rightarrow 0^+$ ground state transition $^{56}\text{Fe}(^{12}\text{C}, ^{10}\text{Be})^{58}\text{Ni}$. The ground state of ^{58}Ni , as discussed above, can be described as $(f_{7/2})^2$ proton configuration considering ^{56}Fe as an inert core. Therefore, in deriving the one-proton transfer probability (P_{1p}), the data for transition to the $f_{7/2}$ single particle state in ^{57}Co were considered. The quantities P_{2p} and $(P_{1p})^2$ are plotted in figure 6(a). The forward angle data for which $\sigma_{\text{el}} = \sigma_R$ were considered. The enhancement factor, defined [4, 12] as the ratio of P_{2p} over $(P_{1p})^2$, has been extracted and has a value between 200 and 60 depending on θ . The enhancement so obtained for the $0^+ \rightarrow 0^+$ ground state transition probably indicates the dominance of a simultaneous transfer over the sequential transfer of two protons at this bombarding energy which, probably, also justifies the analysis of data in terms of DWBA assuming a one-step transfer.

The mechanism of three-nucleon transfer in $^{56}\text{Fe}(^{12}\text{C}, ^9\text{Be})^{59}\text{Ni}$ may involve (a) direct transfer of a ^3He as a cluster, (b) sequential transfer of two protons and a neutron, (c) transfer of a pair of protons followed by transfer of a neutron, and (d) sequential transfer of a deuteron and a proton. One may define a suitable enhancement factor (EF) as detailed below to look for the dominance of ^3He cluster transfer:

$$EF = \frac{P_{^3\text{He}}}{3 \times [(P_{1p})^2 \times (P_{1n})] + 2 \times [(P_{2p}) \times (P_{1n}) + (P_{1d}) \times (P_{1p})]} \quad (1)$$

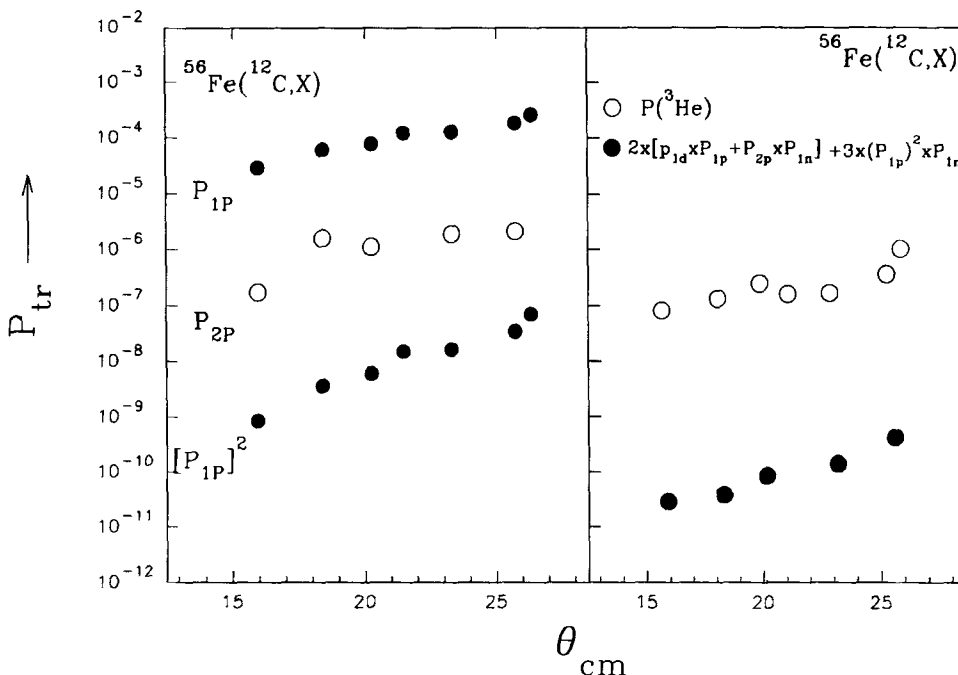


Figure 6. Transfer probability for (a) one and two proton and (b) three nucleon transfer reactions in $^{12}\text{C} + ^{56}\text{Fe}$. See text for details.

The multiplicative factors in the denominator account for all possible combinations of three nucleon transfer.

In the case of ^3He stripping, the data for the ground state transition have been considered for obtaining $P_{^3\text{He}}$. As mentioned above, the peak seen at $E_x \approx 0\text{ MeV}$ in the energy spectrum of ^9Be is due to the addition of the contributions from the states at $E_x = 0.0(\frac{3}{2}^-)$, 343 keV ($\frac{5}{2}^-$) and 468 keV ($\frac{1}{2}^-$) which within the present experimental resolution cannot be resolved. In order to determine the cross-section for a single-transition, DWBA calculations using LOLA were performed for these three transitions assuming a one-step transfer of a ^3He cluster, the cluster being in a $0s$ internal state of motion while being transferred. The DWBA results multiplied by the respective spectroscopic strength were used to determine the contribution from different states to the area under the peak at $E_x \approx 0$. The spectroscopic factors that are used in this calculation are those reported in (d, p) studies [14]. However, studies on ^3He transfer reaction $^{56}\text{Fe}(^6\text{Li}, t)$ indicated [15] that the selectivity observed in transitions to the low-lying states in ^{59}Ni is the same as that observed in the (d, p) reaction and a mechanism in which the two protons are transferred into their lowest orbits while the neutron is transferred into a single particle state was suggested. Thus, the use of the same relative spectroscopic factors for the three nucleon transfer reaction as that obtained from a single neutron transfer study is probably justified.

In the case of sequential transfer of three nucleons, only those specific transitions that may lead to the $\frac{3}{2}^-$ g.s. of ^{59}Ni were considered and the corresponding probabilities were extracted from the present data. A large enhancement factor (figure 6b) of more than

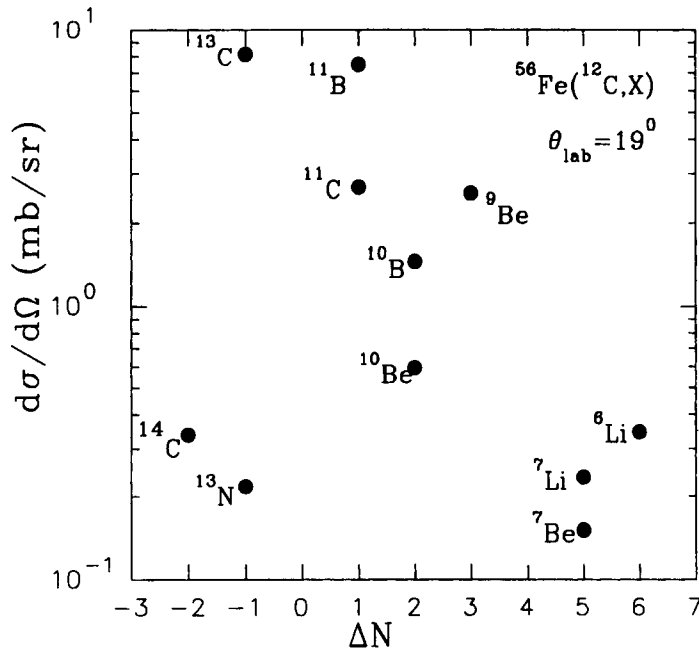


Figure 7. Differential cross-section for all the transfer channels measured in $^{56}\text{Fe}(^{12}\text{C}, X)$ plotted as a function of the number of nucleons transferred (ΔN). The negative values of ΔN correspond to pick up channels.

1000 is obtained at all the angles indicating the dominance of a ^3He cluster transfer over the sequential transfer of three nucleons.

The cluster transfer of ^3He from the projectile to the target nucleus is also clearly evident in figure 7 where the measured cross-section of different transfer products is plotted as a function of the number of transferred nucleons (ΔN). It is observed that, the single nucleon transfer cross-section, as expected, is the largest and, in general, the cross-section decreases as ΔN increases. A strong exception is the ^9Be outgoing channel where a relatively large cross-section has been noticed. The enhancement in the cross-section in the region $\Delta N = 3$ can be attributed as due to ^3He cluster transfer. The data for four nucleon ($2p2n$) transfer channel, where also a large enhancement in the cross-section is expected due to cluster transfer of α , cannot be extracted from the present measurement as the ^8Be is unbound and requires a coincidence measurement of 2α .

4. Discussion and conclusion

The present study reports on the investigation of two- and three-nucleon transfer reactions $^{56}\text{Fe}(^{12}\text{C}, ^{10}\text{Be})^{58}\text{Ni}$ and $^{56}\text{Fe}(^{12}\text{C}, ^9\text{Be})^{59}\text{Ni}$ at an incident ^{12}C energy about twice the Coulomb barrier. Transitions to the low-lying discrete states in the residual nuclei have been identified and the angular distributions have been measured. The measured angular distribution data for two proton transfer have been analysed using the DWBA and assuming a one-step direct transfer of two protons. The shape of the measured angular

distributions are well reproduced by the DWBA calculations. The two-proton spectroscopic factors for the 2^+ and 4^+ states in ^{58}Ni have been obtained from the present work.

Indirect, two-step mechanism involving the inelastic excitations in either the target or projectile followed by two nucleon transfer may become, in some cases, an important mechanism. The two-step amplitude may interfere either constructively or destructively with the one-step amplitude, resulting in a pronounced but distinctly different interference pattern that is evident, for an example, in the case of [16] $^{186}\text{W}(^{12}\text{C},^{14}\text{C})$ where the 2^+ and 4^+ transitions in ^{184}W show an interference dip. A detailed coupled channel calculation is needed to evaluate, quantitatively, the contribution from such indirect processes in any given transition. However, the present two-proton transfer data do not indicate any such striking difference in the shape of the angular distribution. This observation, together with the fact that a one step DWBA calculation reproduces the experimental angular distribution well indicates that any such two-step processes, probably are not so important in the present cases.

The sequential transfer processes cannot be ruled out and can be a dominant mechanism for reactions between heavy ions. A quantitative estimate of the relative contribution from the two (a two-step sequential transfer and a one-step simultaneous transfer) for a given transition would be difficult. An approach based on the transfer probability considerations has been followed in the present work to emphasise the dominance of one on the other. When the measured transfer probability for the $0^+ \rightarrow 0^+$ ground state transition in $^{56}\text{Fe}(^{12}\text{C},^{10}\text{Be})^{58}\text{Ni}$ is compared with the probability for sequential transfer of two protons in the corresponding single particle orbits, a large enhancement for the ratio of $P_{2p}/(P_{1p})^2$ is observed indicating that, probably, a one-step direct transfer mechanism dominates at this bombarding energy and also justifies the analysis of data in terms of a one-step DWBA.

The transfer probability analysis has been extended to the three nucleon transfer reaction $^{56}\text{Fe}(^{12}\text{C},^9\text{Be})^{59}\text{Ni}$. A relatively large cross-section has been measured for this channel. A comparison of transfer probabilities between the various processes that may lead to the ground state of ^{59}Ni seems to suggest that the transition prefers to proceed through a one-step ^3He cluster transfer rather than through a sequential transfer of nucleons.

Acknowledgements

The authors would like to thank H C Jain and M L Jhingan for help during the experiment and many discussions. The co-operation and excellent support of the operational staff of the Pelletron accelerator is greatly appreciated. It is pleasure to thank D H Dias and D C Ephraim of the target laboratory for the help rendered in preparing thin targets at short notice.

References

- [1] W Von Oertzen, Nuclear collision from the mean-field into the fragmentation regime, *Proc. "Enrico Fermi" CXII* p. 459 (1991)
- [2] L G Moretto and R Schmitt, *J. de Phys. Colloq.* 37 **C5**, 109 (1976)
- [3] B J Roy, M G Betigeri, H C Jain and M L Jhingan, *Nucl. Phys.* **A564**, 271 (1993)

Multi-nucleon transfer reactions

- [4] B J Roy, B Srinivasan, E Shallom, M G Betigeri, H C Jain and M L Jhingan, *Nucl. Phys.* **A588**, 706 (1995)
- [5] B J Roy, B Srinivasan, M G Betigeri, H C Jain and M L Jhingan, *Nucl. Phys.* **A597**, 151 (1996)
- [6] D Evers, W Assmann, K Rudolph, S J Skorka and P Sperr, *Nucl. Phys.* **A198**, 268 (1972)
- [7] W P Alford, R A Lindgren, D Elmore and R N Boyd, *Nucl. Phys.* **A243**, 269 (1975)
- [8] L K Peker, *Nuclear Data Sheets* **61**, 189 (1990)
- [9] C M Baglin, *Nuclear Data Sheets* **69**, 733 (1993)
- [10] P Schwandt, IUCF Report 84-X (1984)
- [11] S Cohen and D Kurath, *Nucl. Phys.* **A141**, 145 (1970)
- [12] C Y Wu, W Von Oertzen, D Cline, G W Guidry, *Ann. Rev. Nucl. Part. Sci.* **40**, 285 (1990)
- [13] W Von Oertzen, in *Proc. Int. School on Physics*, Enrico Fermi, edited by C Detraz and P Kienle, 1991
- [14] M S Chowdhury and H M Sen Gupta, *Nucl. Phys.* **A205**, 454 (1973)
- [15] C W Woods, N Stein and J W Sunier, *Phys. Rev.* **C17**, 66 (1978)
- [16] K A Erb, D L Hanson, R J Ascutto, B Sorensen, J S Vaagen and J J Kolata, *Phys. Rev. Lett.* **33**, 1102 (1974)